Ab Initio Study of the Reaction Mechanisms of NiO and NiS with H_2

Der-Yan Hwang*,† and Alexander M. Mebel*,‡

Department of Chemistry, Tamkang University, Tamsui 25137, Taiwan, and Institute of Atomic and Molecular Sciences, Academia Sinica, P.O. Box 23-166, Taipei 10764, Taiwan

Received: July 11, 2001; In Final Form: November 6, 2001

Singlet and triplet potential energy surfaces for the NiO + H_2 → Ni + H_2O and NiS + H_2 → Ni + H_2S reactions have been investigated by density functional calculations at the B3LYP/6-311+G(3df,2p)//B3LYP/6-31G** level as well as by ab initio CCSD(T), CASSCF, and MRCI calculations for some of the key species. The singlet−triplet intersystem crossing is shown to play a crucial role for both reactions. The reaction of nickel oxide with molecular hydrogen starts from the formation of a t-ONi−H_2 complex bound by 3.7 kcal/mol relative to NiO($^3\Sigma^-$) and H_2. This is followed by an intersystem crossing (the spin−orbit coupling computed at a representative point CI1 of the singlet−triplet intersection is 86 cm^{-1}) and the system proceeds via a barrier of 13.3 kcal/mol (transition state s-TS1) in singlet electronic state to form a HNiOH intermediate in singlet or triplet states. t-HNiOH, 9.1 kcal/mol more stable than s-HNiOH, lies 44.8 kcal/mol below the reactants. The HNiOH molecule rearranges to a triplet t-Ni−OH_2 molecular complex via transition state s-TS2 on the singlet potential energy surface and via singlet−triplet transitions, whereas the spin−orbit coupling for a crossing point CI2 in the transition state vicinity is evaluated as 27 cm^{-1}. On the last reaction step the complex bound by 3.8 kcal/mol dissociates to Ni(^{3}F) + H_2O without an exit barrier. For the reverse reaction, Ni(^{3}F) + H_2O → t-HNiOH, the barrier, which occurs at s-TS2 in singlet electronic state, is 12.1 and 4.9 kcal/mol at the B3LYP/6-311+G(3df,2p) and CCSD(T)/6-311+G(3df,2p) levels, respectively. The NiS + H_2 reaction begins on the triplet potential energy surface and proceeds via a barrier [transition state t-TS1(S)] of 19.1 kcal/mol relative to NiS($^3\Sigma^-$) + H_2 to produce the global minimum—a triplet HNiSH molecule, 18.2 kcal/mol below the reactants. This intermediate dissociates to the triplet Ni atom and H_2S via s-TS2(S) and a s-Ni−SH_2 complex involving singlet−triplet intersections. The Ni(^{3}F) + H_2S reaction is predicted to rapidly produce the HNiSH molecule, which, in turn, can dissociate to NiS + H_2 overcoming a barrier of ∼13 kcal/mol with respect to the reactants. Since the highest barriers along the NiO + H_2 → Ni + H_2O and NiS + H_2 → Ni + H_2S reaction pathways are ∼13 and ∼19 kcal/mol, molecular hydrogen is expected to reduce nickel oxide and NiS to atomic nickel at elevated temperatures.

1. Introduction

Hydrogen absorption on metals and their compounds has potential for industrial applications. H_2-complexes were synthesized and studied during the 1980s in transition metal compounds.[1,2] Ab initio studies by Valtazanos and Nicolaides showed that H_2 interacts with cations of metal atoms or dimers such as Be^{2+}, B^{2+}, Be^+, Li^+, or Be_2^{2+} to form dihydrogen complexes, e.g., $Be^{2+}(H_2)$, rather than ordinary dihydrides with the simultaneous scission of the H_2 bond.[3,4] The bonding mechanism consists of induced σ bonding with H_2 σ orbital and weak π back-bonding with σ^* orbital of H_2.[5−7] Recently, we found that oxides and sulfides of the alkaline earth metals (for instance, Be) also can form stable molecular complexes with H_2.[8,9] The binding energies in $OBeH_2$ and $SBeH_2$ with respect to the H_2 lost are 15.6 and 12.4 kcal/mol, respectively.[8,9]

The purpose of this paper is to study the hydrogen absorption by transition metal oxides and sulfides, in particular, NiO and NiS, and to investigate the singlet and triplet reaction pathways of these compounds with molecular hydrogen, NiO + H_2 → H_2−NiO → HNiOH → Ni + H_2O and NiS + H_2 → H_2−NiS → HNiSH → Ni + H_2S. The reverse reactions of nickel metals with water and H_2S are also of interest and have been a subject of numerous experimental and theoretical studies.[10−23] The reactions between first row transition metal atoms and water molecules have been studied by Margrave and co-workers[10,11] using matrix-isolation infrared spectroscopy. Among the late transition metals, only Ni atoms were found to undergo an oxidative addition reaction with water in the low-temperature matrix. Further experimental studies by Mitchell et al.[22] confirmed that the oxidative addition product, HNiOH, can be formed at room temperature. Ab initio calculations in the same work[22] clarified the Ni + H_2O reaction mechanism and demonstrated the importance of both triplet and singlet potential energy surfaces. The authors concluded that the presence of the low lying ^{1}D state is responsible for the unique reactivity of nickel, among the late first row transition metal atoms, with respect to the oxidative addition reaction with water. However, the potential energy surfaces of the HNiOH system were not studied completely, in particular, in the direction of the NiO + H_2 products.

The NiO + H_2 → Ni + H_2O reaction is also interesting because it can be related to the transformation of carbon monoxide and molecular hydrogen to formaldehyde. Our recent theoretical study[24] demonstrated that beryllium oxide in the gas phase can catalyze the CO + H_2 → H_2CO reaction by the following

* Corresponding authors.
† Tamkang University.
‡ Academia Sinica.

10.1021/jp012650a CCC: $22.00
Published on Web 12/14/2001

pathway: $BeO + H_2 + CO \rightarrow HBeOH + CO \rightarrow OC(H)BeOH \rightarrow H_2CO + BeO$, so that the carbon atom of CO inserts into a relatively weak Be−H bond and then formaldehyde can be produced by intramolecular hydrogen migration from O to C. It would be interesting to investigate a similar mechanism for a transition metal, and the reaction of NiO with molecular hydrogen represents the first step of this mechanism. In this paper, we report a study of the lowest singlet and triplet potential energy surfaces of the HNiOH and HNiSH systems using various density functional and ab initio methods. After an assessment of the performance of different theoretical methods, the most reliable results are chosen to describe the reaction mechanisms for NiO/NiS + H_2 and the reverse reactions of nickel atoms with water and H_2S.

2. Computational Details

Since the energy difference between the lowest triplet (^{3}F, $3d^84s^2$) and singlet (^{1}D, $3d^94s^1$) electronic states of nickel atom[25] is only 3410 cm^{-1} and the singlet−triplet energy splitting for NiO is 21.7 kcal/mol,[26] both singlet and triplet reaction pathways may be important. Therefore, we consider both singlet and triplet minimum energy pathways for the title reactions. On these surfaces, full geometry optimizations were run to locate all intermediates and transition states at the B3LYP/6-31G** level of theory.[27,28] We used spin-unrestricted B3LYP (UB3LYP) calculations for the triplet state. On the singlet surface both a reactant Ni(^{1}D) and a product NiX($^1\Delta$), X = O and S, have open shell wave functions. Therefore, for intermediates and transition states we carried out calculations for open and closed shell singlet states using the UB3LYP and spin-restricted RB3LYP methods, respectively, then compared their energies and chose the species with lower energies to draw the potential energy surface for the lowest singlet state. In these cases we carried out both RB3LYP and UB3LYP geometry optimizations. The harmonic vibrational frequencies were obtained at the B3LYP/6-31G** level in order to characterize the stationary points as local minima or first-order saddle points, to obtain zero-point vibrational energy corrections (ZPE), and to generate force constant data needed in the IRC calculation. The intrinsic reaction coordinate IRC method[30] was used to track minimum energy paths from transition structures to the corresponding local minima. A step size of 0.1 $amu^{1/2}$ bohr or larger was used in the IRC procedure. The relative energies were refined at the B3LYP/6-31G** optimized geometries using the B3LYP/6-311G**, B3LYP/6-311+G(3df,2p), and CCSD(T)/6-311+G(3df,2p) methods.[31] Various electronic states of the Ni atom and NiO were also calculated using multireference CASSCF[32] and MRCI[33] methods with the full valence active space. The choice of the most reliable approximation is discussed in the next section.

Most of the ab initio calculations described here were carried out employing the Gaussian 98 program[34] and for some of them the MOLPRO 2000 package[35] was used.

3. Results and Discussion

The calculated singlet−triplet energy gaps for Ni and NiO and the Ni−O bond strength are shown in Table 1. The relative energies and ZPE of various compounds in the reaction of NiO + H_2 computed at different levels of theory are listed in Table 2. Table 3 presents calculated vibrational frequencies. The potential energy diagram along the reaction pathway computed at the B3LYP/6-311+G(3df,2p)//B3LYP/6-31G** + ZPE-[B3LYP/6-31G**] level is shown in Figure 1. The optimized geometries of various species along the predicted pathway of the NiO + H_2 reaction are depicted in Figures 2 and 3. For the NiS + H_2 reaction, the relative energies and ZPE of various compounds at different levels of theory are listed in Table 4 and Table 5 shows calculated vibrational frequencies. The potential energy diagram along the NiS + H_2 reaction path computed at the B3LYP/6-311+G(3df,2p)//B3LYP/6-31G** + ZPE[B3LYP/6-31G**] level is presented in Figure 4. The optimized structures of various intermediates and transition states of the NiS + H_2 reaction are drawn in Figures 5 and 6.

TABLE 1: Singlet−Triplet Energy Differences for Ni and NiO and the Ni−O Bond Strength in the Ground State NiO, $^3\Sigma^-$, (kcal/mol) Calculated at Different Levels of Theory

method	Ni, ^{3}F−^{1}D	NiO, $^3\Sigma^-$−$^1\Delta$	NiO, $^3\Sigma^-$−$^1\Sigma^+$	Ni−O bond
B3LYP/6-31G*	19.5	10.5	35.1	81.8
B3LYP/6-311G*	18.4	14.9	35.9	70.0
B3LYP/6-311+G(3df)	3.0	10.6	33.9	83.9
CCSD/6-311G*	16.4	21.1	28.5	47.1
CCSD/6-311+G(3df)	5.1	26.7	28.1	68.7
CCSD(T)/6-311G*	9.5	29.9	15.1	64.2
CCSD(T)/6-311+G(3df)	1.5	35.8	16.7	87.2
CASSCF[a]/6-311+G(3df)	7.1	18.5	39.5	116.9
MRCI[a]/6-311+G(3df)	6.7	23.7	33.4	61.7
MRCI+Q[a]/6-311+G(3df)	6.3	26.0	34.8	75.1
experiment	9.7[b]	21.7[c]	41.5[c]	90.4[d]

[a] Full-valence active space calculations; the active space is (10,6) for Ni, (16,10) for NiO, and (6,4) for O. [b] From ref 25. [c] From ref 26. [d] From ref 40.

A. Assessment of Computational Methods. Let us first compare the performance of different methods for the singlet−triplet splitting in the Ni atom and NiO and for the strength of the Ni−O bond related to the reaction energetics. The singlet−triplet energy gap for the Ni atom (between the ^{3}F ($3d^84s^2$) and ^{1}D ($3d^94s^1$) states), 9.7 kcal/mol in experiment,[25] is difficult to reproduce by single-reference-based ab initio methods. As seen in Table 1, at the UCCSD(T)/6-311+G(3df) level this energy is computed as 1.5 kcal/mol, while the UCCSD(T)/6-311G** calculations fortuitously give the ^{3}F−^{1}D energy gap very close to experiment. Density functional UB3LYP/6-311+G(3df) calculations result in 3.0 kcal/mol but UB3LYP with the smaller 6-31G* and 6-311G* basis sets give the energy of the ^{1}D ($3d^84s^2$) singlet state lower than ^{1}D ($3d^94s^1$) (by 41.8 kcal/mol at B3LYP/6-31G*), so the comparison of their results with those by other methods is not warranted. Full-valence active space CASSCF and MRCI/6-311+G(3df) calculations for the Ni atom result in 6.3−7.1 kcal/mol for the singlet−triplet energy difference, in a reasonable agreement with the experimental value.

Various electronic states of NiO have been investigated both experimentally and theoretically.[26,36] The B3LYP/6-31G* calculations give the bond length in the $^3\Sigma^-$ state as 1.601 Å, slightly shorter than that in experiment, 1.627 Å.[36] Mention that the most sophisticated so far MR-ACPF calculations by Bauschlicher and Maitze[37] also resulted in 1.601 Å, density functional BP86 calculations by Citra et al.[38] gave a slightly longer bond length of 1.644 Å, while BLYP calculations by Doll et al.[39] provided the best agreement with experiment (1.626 Å). The B3LYP method somewhat overestimates the vibrational frequency of the $^3\Sigma^-$ state, 926 cm^{-1} vs experimental 842.6 cm^{-1}.[38] For the frequency, the best results were obtained by Bauschlicher and Maitze[37] (850 cm^{-1}) and by Citra et al.[38] (823 cm^{-1}), and the BLYP frequency[39] (897 cm^{-1}) is quite close to our B3LYP value. For the lowest singlet $^1\Delta$ state, the B3LYP/6-31G* computed bond length and frequency are 1.576 Å and 1004 $cm,^{-1}$ respectively, while the frequency obtained in experiment is much lower, 680 cm^{-1}.[26] The difference can be reduced by

TABLE 2: ZPE Corrected Relative Energies (kcal/mol) Calculated at Different Levels of Theory for Various Compounds in the Reaction of NiO with H_2

		B3LYP			CCSD(T)
species	ZPE[a]	6-31G**	6-311G**	6-311+G(3df,2p)	6-311+G(3df,2p)
s-NiO($^1\Delta$) + H_2	7.82	10.53	14.93	10.61	35.85
s-ONi−H_2[b]					
RB3LYP/6-31G**	10.84	5.47	14.25	15.34	3.58
UB3LYP/6-31G**, $\langle S^2\rangle = 0.920$	10.86	−1.68	2.84	4.49	
s-TS1[b]					
RB3LYP/6-31G**	9.38	17.63	23.70	19.92	13.27
UB3LYP/6-31G**, $\langle S^2\rangle = 0.764$	9.10	12.84	17.96	13.28	
s-HNiOH[b]					
RB3LYP/6-31G**	12.02	−29.73	−35.20	−33.05	−32.39
UB3LYP/6-31G**, $\langle S^2\rangle = 0.928$	11.35	−42.26	−42.18	−35.66	
s-TS2[b]					
RB3LYP/6-31G**	11.34	6.63	−9.30	−17.81	−19.76
UB3LYP/6-31G**, $\langle S^2\rangle = 0.781$	10.89	−9.93	−13.03	−17.04	−11.67
s-Ni−OH_2[b]					
RB3LYP/6-31G**	14.28	6.90	−14.93	−25.57	−37.59
UB3LYP/6-31G**, $\langle S^2\rangle = 1.007$	14.59	−15.74	−27.38	−27.78	−25.27
s-Ni(^{1}D) + H_2O	13.41	−1.63	−19.20	−26.94	−23.16
t-NiO($^3\Sigma^-$) + H_2[c]	7.71	0	0	0	0
t-ONi−H_2	10.32	−9.76	−6.71	−3.71	−4.13
t-TS1	7.65	4.14	−6.00	19.14	23.98
t-HNiOH	10.77	−56.75	−52.84	−44.77	−41.82
t-TS2	10.47	−8.81	−3.10	−6.58	0.14
t-Ni−OH_2	14.50	−30.53	−40.57	−33.67	−32.05
t-Ni(^{3}F) + H_2O	13.41	−21.14	−37.58	−29.93	−24.63

[a] Zero-point energies are calculated at the B3LYP/6-31G** level. [b] Optimized at different levels of theory shown below. ZPE are calculated at the same level as the geometry optimization. [c] The total energies of t-NiO + H_2 are the following: B3LYP/6-31G**: −1584.43037, B3LYP/6-311G**: −1584.58271, B3LYP/6-311+G(3df,2p): −1584.65732, and CCSD(T)/6-311+G(3df,2p): −1583.37395.

TABLE 3: Vibrational Frequencies (cm^{-1}) of Various Compounds in the NiO + H_2 Reaction through the Singlet and Triplet Pathways Calculated at the B3LYP/6-31G Level**

species	frequencies
s-NiO($^1\Delta$)	1004
s-ONi−H_2	
RB3LYP/6-31G**	339, 773, 981, 1105, 1967, 2415
UB3LYP/6-31G**	305, 490, 940, 1047, 1687, 3125
s-TS1	
RB3LYP/6-31G**	1007i, 508, 911, 989, 1970, 2187
UB3LYP/6-31G**	807i, 481, 819, 916, 1780, 2370
s-HNiOH	
RB3LYP/6-31G**	380, 547, 803, 812, 2094, 3773
UB3LYP/6-31G**	350, 480, 628, 748, 1880, 3857
s-TS2	
RB3LYP/6-31G**	989i, 621, 700, 1146, 1832, 3636
UB3LYP/6-31G**	1248i, 584, 639, 959, 1720, 3716
s-Ni−OH_2	
RB3LYP/6-31G**	411, 438, 574, 1546, 3469, 3552
UB3LYP/6-31G**	357, 402, 474, 1600, 3627, 3746
t-NiO($^3\Sigma^-$)	926
t-ONi−H_2	235, 280, 793, 967, 1532, 3412
t-TS1	851i, 212, 357, 849, 1916, 2015
t-HNiOH	189, 323, 451, 769, 1890, 3708
t-TS2	1152i, 605, 609, 795, 1579, 3734
t-Ni−OH_2	299, 379, 452, 1609, 3642, 3763

using the B3LYP and BLYP density functionals with the large 6-311+G(3df) basis which give a longer Ni−O bond length, 1.626 and 1.644 Å, and a lower frequency, 861 and 814 cm^{-1}, respectively. However, the deviations of the calculated frequencies from experiment, though significant for spectroscopy, do not affect the energetics of NiO much, since the differences in ZPE are small.

According to photoelectron spectroscopic measurements by Wu and Wang,[26] the two lowest singlet states of nickel oxide are $^1\Delta$ and $^1\Sigma^+$, which, respectively, lie 21.7 and 41.5 kcal/mol above the ground $^3\Sigma^-$ state. As seen Table 1, these values are not accurately reproduced even by sophisticated ab initio calculations. For instance, B3LYP calculations with various basis sets gave the $^3\Sigma^- - ^1\Delta$ and $^3\Sigma^- - ^1\Sigma^+$ energy differences as 10−15 and 34−36 kcal/mol, significantly underestimating the experimental results. The CCSD method overestimates the $^3\Sigma^- - ^1\Delta$ splitting by ∼5 kcal/mol but underestimates $^3\Sigma^- - ^1\Sigma^+$ by ∼13 kcal/mol. When triple excitations are included as perturbation, the agreement with experiment drastically worsens; at CCSD(T) levels two singlet states switch their order and $^1\Sigma^+$ and $^1\Delta$ are calculated to lie 15−17 and 30−36 kcal/mol higher than the ground triplet state. Although the CASSCF calculations give the singlet−triplet energy gaps as 18.5 and 39.5 kcal/mol, close to experiment, the higher level MRCI/6-311+G(3df) approximation overestimates the $^1\Delta$ energy and underestimates $^1\Sigma^+$.

In experiment, the bond strength in the ground-state nickel oxide is 90.4 kcal/mol.[40] The bond strength calculated at the CCSD(T)/6-311+G(3df) level with ZPE correction based on the experimental vibrational frequency is 87.2 kcal/mol, close to the MR-ACPF result by Bauschlicher and Maitze[37] (87.6 kcal/mol) and in reasonable agreement with experiment. B3LYP/6-311+G(3df) calculations give a slightly underestimated value of 83.9 kcal/mol, while CCSD(T) and B3LYP with the 6-311G* basis sets give the results more than 20 kcal/mol too low as compared to experiment. Based on the experimental heats of formation for the Ni atom (102.8 kcal/mol) and oxygen (59.6 kcal/mol),[41] ΔH_f for NiO is 72.0 kcal/mol. Using this value and experimental ΔH_f for Ni and H_2O (−57.8 kcal/mol),[41] one can see that the NiO + H_2 → Ni + H_2O reaction is exothermic by 27.0 kcal/mol. The B3LYP/6-311G* and CCSD(T)/6-311G* methods overestimate this value by 10.6 and 10.9 kcal/mol, respectively. The B3LYP/6-311+G(3df) and CCSD(T)/6-311+G(3df,2p) calculations result in ΔH_f = 29.9 and 24.6 kcal/mol, respectively, within a 2−3 kcal/mol error margin from experiment.

The above comparisons show that the B3LYP/6-311+G(3df,2p)//B3LYP/6-31G** approach seems to be a reasonable

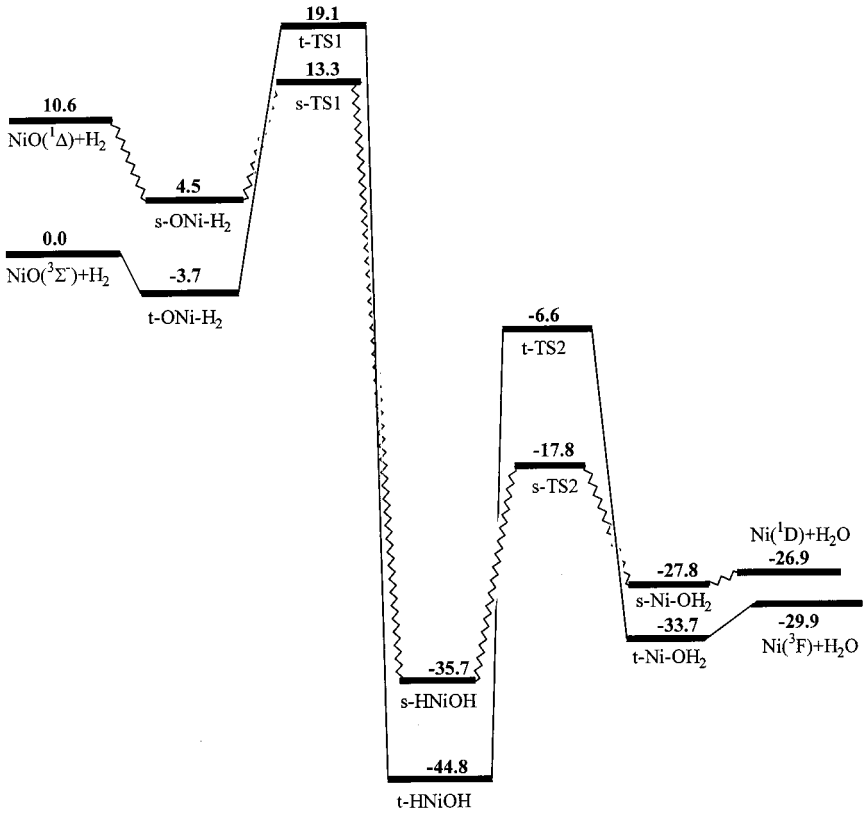

Figure 1. Potential energy diagram for the NiO + H_2 → Ni + H_2O reaction calculated at the B3LYP/6-311+G(3df,2p)//B3LYP/6-31G** + ZPE(B3LYP/6-31G**) level.

compromise between the cost and accuracy for the description of the NiO/NiS + H_2 → Ni + H_2O/H_2S reactions, although we have to keep in mind that for the species at the initial reaction steps the energy differences between triplet and singlet states are underestimated. Much more expensive CCSD(T)/6-311+G-(3df,2p) calculations may be more accurate for the triplet PES but are not reliable for the initial steps at the singlet surface since they fail to properly describe the $^3\Sigma^- - ^1\Delta$ energy gap and to give the correct energetic order of the singlet states of NiO.

B. NiO + H_2 Reaction Mechanism. *Triplet Potential Energy Surface.* As seen in Figures 1 and 3, at the first stage of the NiO + H_2 reaction in triplet electronic state the H_2 molecule attaches to the Ni atom of NiO to form a molecular t-ONi−H_2 complex of C_s geometry without a barrier. The structure of t-ONi−H_2 (^{3}A") is not planar. The t-ONi−H_2 complex conserves the molecular structure of H_2 with slightly stretched HH bond (R_{HH} = 0.805 Å) and two hydrogen atoms have equal distances from the nickel atom, 1.641 Å. The nonplanar geometry of the complex can be rationalized in terms of the scheme of σ donation and π back-donation from the σ and σ^* orbitals of H_2 and molecular orbital diagram of NiO.[26] The electronic configuration of NiO($^3\Sigma^-$) is $1\sigma^2 1\pi^4 1\delta^4 2\sigma^2 2\pi^2$. The σ donation occurs from the occupied σ orbital of H_2 to the empty 3σ orbital of NiO and does not depend on the planarity of the mutual orientation of the two molecules. On the other hand, the π back-donation involves the empty σ^* orbital of H_2 and two degenerate perpendicular singly occupied 2π orbitals of NiO. If NiO and H_2 lie in the same plane, the π back-donation can occur only from one (in-plane) π orbital, while the nonplanar arrangement allows the π back-donation from both π orbitals. The B3LYP/6-311+(3df,2p) calculated energy of the complex formation is 3.7 kcal/mol. From the t-ONi−H_2 complex, the reaction proceeds by migration of one of the hydrogen atoms

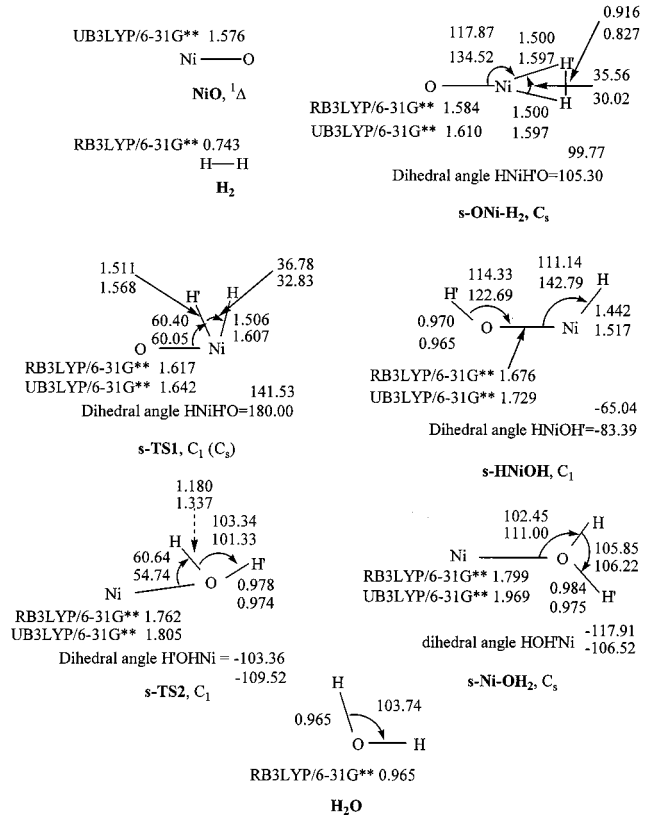

Figure 2. Geometries of the reactants, products, intermediates, and transition states of the NiO + H_2 → Ni + H_2O reaction in the singlet electronic state, optimized at the UB3LYP and RB3LYP levels of theory with the 6-31G** basis set. (Bond lengths are in angstroms and bond angles are in degrees.)

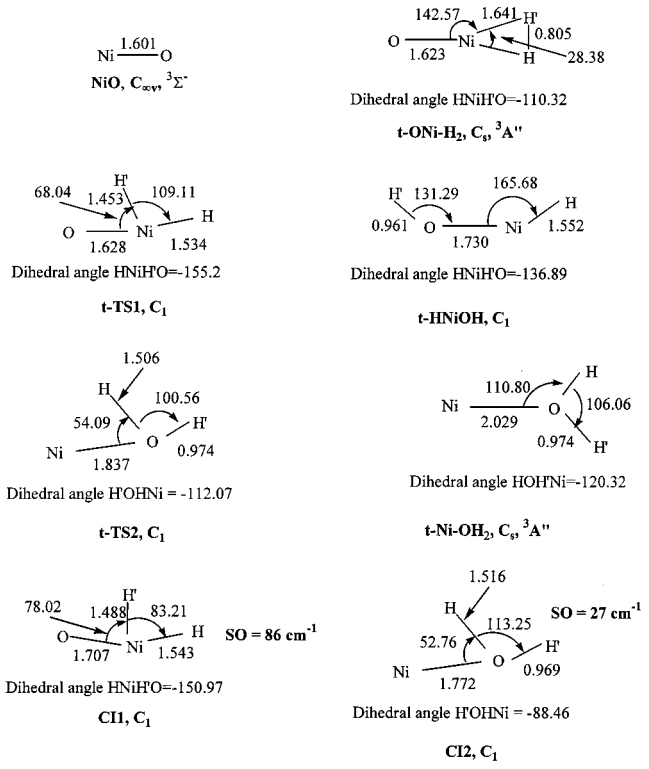

Figure 3. Geometries of the reactants, products, intermediates, and transition states of the NiO + H_2 → Ni + H_2O reaction in triplet electronic state, optimized at the UB3LYP/6-31G** level of theory, and structures of representative points (CI1 and CI2) on the singlet−triplet intersection surface calculated at the CASSCF(18,12)/6-311G** level. (Bond lengths are in angstroms and bond angles are in degrees.)

to produce a nonplanar nonlinear intermediate t-HNiOH via transition state t-TS1. From t-ONi−H_2 to t-TS1 the ONiH angle bends from 142.6° to 68.0°, the ONi bond elongates by only 0.005 Å, two hydrogen atoms become separated from each other (2.433 Å), and a new O−H bond begins to form (1.730 Å). The B3LYP/6-311+(3df,2p) calculated barrier is 22.8 and 19.1 kcal/mol relative to t-ONi−H_2 and the reactants, respectively. The transition state optimization was followed by the frequency and IRC calculations at the B3LYP/6-31G** level of theory, which confirmed that t-TS1 does connect t-ONi−H_2 and the t-HNiOH intermediate.

The t-ONi−H_2 → t-HNiOH reaction step is found to be exothermic by 41.1 kcal/mol and t-HNiOH is stabilized with respect to NiO($^3\Sigma^-$) and H_2 by 44.8 kcal/mol. Mitchell et al.[22] reported a planar structure with a linear ONiH fragment for the t-HNiOH molecule in the $^3A'$ electronic state obtained at the MCPF level of theory. The present B3LYP/6-31G** calculations gave quite similar geometric parameters but ONiH slightly deviates from linearity and the molecule becomes nonplanar. In our B3LYP/6-311+G(3df,2p) and CCSD(T)/6-311+G-(3df,2p) calculations, t-HNiOH lies 14.9 and 17.2 kcal/mol, respectively, below Ni(^{3}F) + H_2O, while Mitchell et al.[22] reported the value of 23.1 kcal/mol for this binding energy. From t-HNiOH, the reaction can continue to form a t-Ni−OH_2 complex via a nonplanar transition state t-TS2. The calculated B3LYP/6-311+(3df,2p) energy places transition state t-TS2 38.2 kcal/mol higher than t-HNiOH. The B3LYP/6-31G** IRC calculation confirmed that the first-order saddle point t-TS2 connects the t-HNiOH intermediate and the t-Ni−OH_2 complex.

Mitchell et al.[22] reported a planar structure of t-Ni−OH_2 of C_{2v} symmetry. In our calculations, the geometry deviates from planarity and only C_s symmetry is conserved. The geometric parameters of the complex optimized at the B3LYP/6-31G** level are very close to those obtained by Fournier[23] who used another version of DFT. At the B3LYP/6-311+G(3df,2p) level, the complex is stabilized with respect to triplet Ni atom and water by 3.8 kcal/mol and can dissociate without an exit barrier.

TABLE 4: ZPE Corrected Relative Energies (kcal/mol) Calculated at Different Levels of Theory for Various Compounds in the Reaction of NiS with H_2

		B3LYP		
species	ZPE[a]	6-31G**	6-311G**	6-311+G(3df,2p)
s-NiS($^1\Delta$) + H_2	7.19	7.53	8.26	8.96
s-SNi−H_2[b]				
RB3LYP	10.17	5.51	10.14	9.65
UB3LYP, $\langle S^2\rangle = 1.010$	9.79	−12.21	−9.01	0.13
s-TS0(S)[c]	7.80	5.98	12.45	20.27
s-SNiH_2[c]	7.98	6.14	13.09	20.19
s-TS1(S)[c]	8.02	6.19	13.11	20.18
s-HNiSH[b]				
RB3LYP	9.55	−8.50	−13.08	−12.45
UB3LYP, $\langle S^2\rangle = 0.978$	9.22	−21.49	−17.00	−9.51
s-TS2(S)[b]				
RB3LYP	9.50	38.47	22.65	1.37
UB3LYP, $\langle S^2\rangle = .005$	9.68	18.93	13.72	8.50
s-Ni−SH_2[b]				
RB3LYP	10.88	35.25	21.02	0.26
UB3LYP, $\langle S^2\rangle = 1.000$	10.56	15.88	11.67	2.86
s-Ni(^{1}D) + H_2S	9.48	19.79	13.74	8.95
t-NiS($^3\Sigma^-$) + H_2[d]	7.16	0	0	0
t-SNi−H_2	9.82	−15.10	−9.36	−3.16
t-TS1(S)	7.23	2.27	21.25	19.11
t-HNiSH	8.93	−35.67	−28.49	−18.19
t-TS2(S)	8.12	6.25	7.10	8.60
t-Ni(^{3}F) + H_2S	9.48	0.30	−4.63	5.95

[a] Zero-point energies calculated at the B3LYP/6-31G** level. [b] Geometry was optimized at the RB3LYP and UB3LYP levels with the 6-31G** basis set. [c] Both UB3LYP and RB3LYP calculations converge to the same closed shell singlet wave function. [d] The total energies of t-NiS + H_2 are the following: B3LYP/6-31G**: −1907.44179, B3LYP/6-311G**: −1907.61512, and B3LYP/6-311+G(3df,2p): −1907.68549.

TABLE 5: Vibrational Frequencies (cm^{-1}) of Various Compounds in the NiS + H_2 Reaction through the Singlet and Triplet Pathways Calculated at the B3LYP/6-31G Level**

species	frequencies
s-NiS($^1\Delta$)	510
s-SNi−H_2	
RB3LYP	293, 553, 673, 1137, 1904, 2550
UB3LYP	177, 306, 435, 1141, 1665, 3128
s-TS0(S)	201i, 182, 430, 581, 2121, 2139
s-SNiH_2	48, 247, 493, 584, 2093, 2119
s-TS1(S)	101i, 322, 508, 585, 2083, 2110
s-HNiSH	
RB3LYP	421, 440, 502, 587, 2099, 2628
UB3LYP	397, 417, 488, 582, 1895, 2670
s-TS2(S)	
RB3LYP	809i, 406, 667, 1084, 2162, 2328
UB3LYP	604i, 217, 446, 1173, 2473, 2497
s-Ni−SH_2	
RB3LYP	430, 616, 618, 1211, 2319, 2418
UB3LYP	279, 340, 464, 1192, 2536, 2553
t-NiS($^3\Sigma^-$)	540
t-SNi−H_2	152, 384, 467, 1037, 1563, 3264
t-TS1(S)	626i, 284, 341, 464, 1869, 2100
t-HNiSH	347, 387, 398, 586, 1860, 2672
t-TS2(S)	445i, 290, 438, 821, 1473, 2658

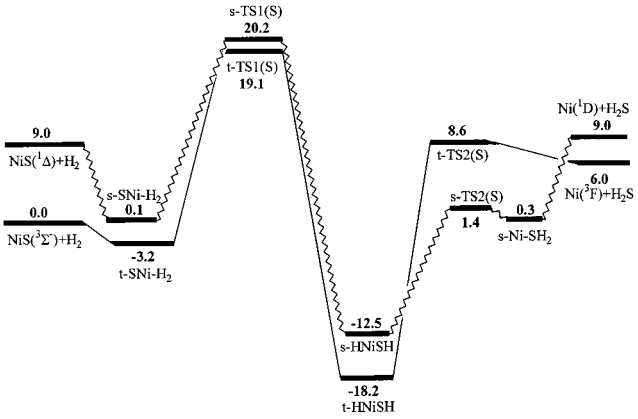

Figure 4. Potential energy diagram for the NiS + H_2 → Ni + H_2S reaction calculated at the B3LYP/6-311+G(3df,2p)//B3LYP/6-31G** + ZPE(B3LYP/6-31G**) level.

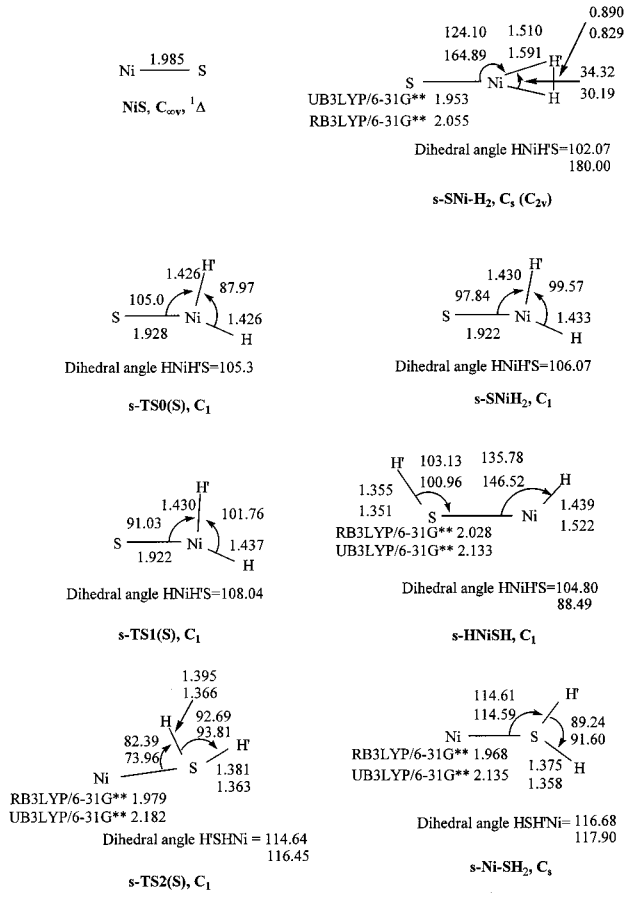

Figure 5. Geometries of the reactants, products, intermediates, and transition states of the NiS + H_2 → Ni + H_2S reaction in singlet electronic state, optimized at the UB3LYP and RB3LYP levels of theory with the 6-31G** basis set. (Bond lengths are in angstroms and bond angles are in degrees.)

The CCSD(T)/6-311+G(3df,2p) complex formation energy, 7.4 kcal/mol, is very close to the value of 7.2 kcal/mol obtained by Mitchell et al.[22]

Singlet Potential Energy Surface. The first stage of the NiO + H_2 reaction in the singlet electronic state is the attachment of the H_2 molecule to the Ni atom of singlet NiO to form a nonplanar s-ONi−H_2 complex of C_s geometry without a barrier. The structure of s-ONi−H_2 shown in Figure 2 is similar to that of t-ONi−H_2, but the Ni−H bonds are 0.044 Å shorter, the H−H bond is 0.022 Å longer, and the deviation from planarity is

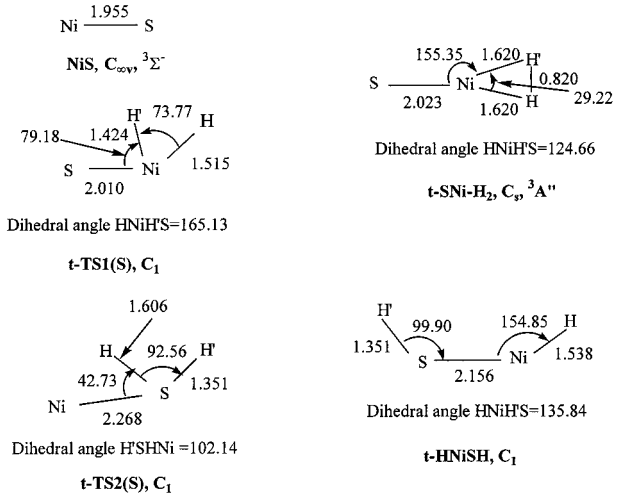

Figure 6. Geometries of the reactants, products, intermediates, and transition states of the NiS + H_2 → Ni + H_2S reaction in triplet electronic state, optimized at the UB3LYP/6-31G** level of theory. (Bond lengths are in Å and bond angles are in degrees.)

stronger. In the lowest singlet state the complex has an open shell wave function; the UB3LYP/6-311+G(3df,2p)//UB3LYP/6-31G** energy is 10.9 kcal/mol lower than the RB3LYP/6-311+G(3df,2p)//RB3LYP/6-31G** energy. The $\langle S^2 \rangle$ value at the UB3LYP level is 0.92 before annihilation of higher spin contributions in the wave function but decreases to ∼0.02 after the annihilation, indicating that the spin contamination is not very severe. The same is true for other open shell singlet $NiOH_2$ intermediates and transition states; their UB3LYP $\langle S^2 \rangle$ values are in the range of 0.75−1.00 before annihilation and 0.02−0.05 after annihilation of higher spin contributions. The singlet complex formation energy, 6.1 kcal/mol at the B3LYP/6-311+G(3df,2p) level, is somewhat higher than that for t-ONi−H_2.

From the complex, the reaction proceeds by migration of one of the hydrogen atoms to form a nonplanar nonlinear intermediate s-HNiOH via a planar transition state s-TS1. Both s-HNiOH and s-TS1 have an open shell character in the lowest singlet state. From s-ONi−H_2 to s-TS1 the ONiH angle bends from 134.5° to 60.1°, the ONi bond slightly shortens and two hydrogen atoms are still close to each other (0.898 Å). Thus, s-TS1 has a much earlier character than t-TS1 on the triplet surface. Also, the singlet transition state lies 5.8 kcal/mol lower than the triplet one and 2.7 kcal/mol above the $NiO(^1\Delta)$ + H_2 reactants. The barrier with respect to the s-ONi−H_2 complex is calculated as 8.8 kcal/mol at the B3LYP/6-311+G(3df,2p) level. The s-ONi−H_2 → s-HNiOH reaction step is found to be exothermic by 31.2 kcal/mol. The s-HNiOH intermediate is 9.1 kcal/mol less stable than t-HNiOH. Interestingly, the difference between the UB3LYP/6-311+G(3df,2p)//UB3LYP/6-31G** and RB3LYP/6-311+G(3df,2p)//RB3LYP/6-31G** energies of s-HNiOH is only 2.6 kcal/mol indicating that two singlet electronic states of this molecule, one with an open shell character and another with a closed shell wave function, lie close to each other. From s-HNiOH, the reaction proceeds to the s-Ni−OH_2 complex via a nonplanar transition state s-TS2. In s-TS2, the open and closed shell singlet state energies are also similar, but in this case the closed shell energy is 0.8 kcal/mol lower at the B3LYP/6-311+G(3df,2p)//B3LYP/6-31G** level. The calculated barrier at s-TS2 is 17.9 kcal/mol relative to s-HNiOH. The Ni−OH_2 complex in the open shell singlet electronic state is 5.9 kcal/mol less favorable than t-Ni−OH_2 and is stabilized by only 0.9 kcal/mol with respect

to the Ni(^{1}D) + H_2O products, which can be produced from the complex without an exit barrier. It is worth mentioning that earlier MCPF calculations[22] gave the triplet Ni−OH_2 energy 3.4 kcal/mol lower than for the singlet state, where the latter was computed at the triplet equilibrium geometry.

Singlet−Triplet Intersystem Crossing. Both transition states on the reaction pathway from NiO + H_2 to Ni + H_2O have lower energies in the singlet electronic state than in the triplet state. On the other hand, the reactants, intermediates, and products show lowest energies in the triplet state. This indicates that the singlet−triplet intersystem crossing can play an important role in the reaction mechanism and make the ground-state triplet reaction more efficient by reducing the barriers. Therefore, we tried to find representative points on the surface of singlet−triplet intersection in the vicinity of TS1 and TS2 and calculate spin−orbit couplings at these points. For the calculations, we used the full valence active space CASSCF-(18,12)/6-311G** method. The search for the singlet−triplet intersection structures was performed using the SEAM program written by Morokuma and co-workers.[42] The spin−orbit coupling calculations were carried out employing the algorithm implemented in the MOLPRO 2000 program.[35]

The geometries of the singlet−triplet crossing points in the vicinity of TS1 (CI1) and TS2 (CI2) are shown in Figure 3. The nonplanar CI1 has the NiH bond lengths (1.49 and 1.54 Å) and HNiH bond angle (83.2°) intermediate between those for s- and t-TS1, 1.57 and 1.61 Å vs 1.45 and 1.53 Å for the bond lengths and 32.8° vs 109.1° for HNiH. On the other hand, the NiO bond length (1.71 Å) and NiOH angle (78.0°) are larger than the corresponding values both in triplet and singlet TS1. The spin−orbit coupling at CI1 is computed as 86 cm^{-1} indicating that the intersystem crossing can be quite efficient at this point of intersection. The structure of CI2 is rather similar to that of t-TS2, except for a larger HOH angle, 113.3° vs 100.6° in the transition state, and slightly shorter NiO distance, 1.77 Å vs 1.84 Å in t-TS2. The calculated spin−orbit coupling at the CI2 crossing point is 27 cm^{-1}, about three times lower than that at CI1. The calculations confirm that the singlet−triplet intersystem crossing can indeed take place along the reaction course not far from the transition state regions, although in the vicinity of TS2 it is expected to be less efficient than near TS1.

Overall Reaction Mechanism. The reaction of the nickel oxide with molecular hydrogen may involve both triplet and singlet potential energy surfaces. The minimal energy reaction pathway, assuming that the singlet−triplet intersystem crossing is efficient, is the following. The reaction starts from the formation of the t-ONi−H_2 complex from NiO($^3\Sigma^-$) and H_2. Then, an intersystem crossing takes place, and the system proceeds via the barrier at s-TS1 in the singlet electronic state. The barrier height is only 13.3 kcal/mol relative to the triplet reactants. If the intersystem crossing would not occur, the reaction has to go over the barrier of 19.1 kcal/mol at t-TS1. Next, the HNiOH intermediate is formed in a singlet or triplet state. t-HNiOH is more stable but its formation would involve another intersystem crossing. The HNiOH molecule rearranges to the triplet t-Ni−OH_2 molecular complex via transition state s-TS2 on the singlet potential energy surface and singlet−triplet intersystem crossing (CI2). The barrier for this reaction step is 27.0 kcal/mol relative to t-HNiOH and 17.9 kcal/mol with respect to s-HNiOH. On the other hand, the isomerization barrier in the triplet state is much higher, 38.2 kcal/mol. Finally, the t-Ni−OH_2 complex dissociates to the most stable products, Ni(^{3}F) + H_2O, without an exit barrier. Overall, the NiO($^3\Sigma^-$) + H_2 → Ni(^{3}F) + H_2O reaction is exothermic by 29.9 kcal/mol (27.0 kcal/mol in experiment)[41] and the highest barrier on the reaction pathway is 13.3 kcal/mol.

For the reverse reaction, Ni(^{3}F) + H_2O → t-HNiOH, the B3LYP/6-311+G(3df,2p) calculated barrier is 12.1 kcal/mol (9.6 kcal/mol without ZPE) occurring at s-TS2 in the singlet electronic state. This result overestimates the classical barrier of 3.1 kcal/mol obtained by Mitchell et al.[22] at the MCPF level. On the other hand, CCSD(T)/6-311+G(3df,2p) calculations give the classical barrier height as 2.8 kcal/mol, close to Mitchell's result. The singlet and triplet surfaces cross along the reaction course at CI2 and the singlet−triplet transition significantly reduces the reaction barrier. It is well-known that such singlet−triplet transitions readily occur in collisional and reactive processes of nickel atoms.[43,44] Our calculations confirm the possibility of the intersystem crossing, though the computed spin−orbit coupling of 27 cm^{-1} for an isolated molecule is not very high. The HNiOH molecule is not likely to dissociate to NiO + H_2 because the barrier is prohibitively high.

C. NiS + H_2 Reaction Mechanism. *Reaction Mechanism.* Our discussion is based on the B3LYP/6-311+G(3df,2p)//B3LYP/6-31G** energies (see Table 4 and Figure 4). At the singlet PES, s-SNi−H_2 as well as NiS($^1\Delta$) and Ni(^{1}D) have the lowest singlet state with an open shell wave function and we consider their UB3LYP energies. All other intermediates and transition states exhibit a closed shell character in the lowest singlet state, therefore, we discuss their RB3LYP energies. At the initial reaction stage the H_2 molecule attaches to the Ni atom of singlet or triplet NiS to form molecular s- or t-SNi−H_2 complexes, respectively, without barrier. In the triplet state, the complex is nonplanar at the B3LYP/6-31G** level and have a structure of C_s symmetry, similar to the geometry of ONi−H_2. On the other hand, the singlet complex is calculated to be planar and has C_{2v} symmetry. The other geometric parameters of s- and t-SNi−H_2 are similar. The complex formation energy in the singlet state, 8.9 kcal/mol, is notably higher than that in the triplet state, only 3.2 kcal/mol.

From the t-SNi−H_2 complex, the reaction proceeds by migration of one of the hydrogen atoms to form a nonplanar nonlinear intermediate t-HNiSH via transition state t-TS1(S). The calculated barriers is 22.3 kcal/mol relative to t-SNi−H_2 and 19.1 kcal/mol with respect to the triplet reactants. The NiS($^3\Sigma^-$) + H_2 → t-HNiSH reaction exothermicity is found to be 18.2 kcal/mol, which is much lower than for the reaction of NiO($^3\Sigma^-$), 44.8 kcal/mol. The transition state optimization was followed by the frequency and IRC calculations at the B3LYP/6-31G** level of theory which confirmed that t-TS1(S) connects t-SNi−H_2 and the t-HNiSH intermediate. The reaction pathway from s-SNi−H_2 to s-HNiSH is found to be more complicated. From the s-SNi−H_2 complex, the reaction first proceeds by changing the HNiH angle and elongating the H−H bond to form s-$SNiH_2$ via transition state s-TS0(S). From s-SNi−H_2 to s-TS0(S) the SNiH angle bends from 124.1° to 105.0°, the SNi bond slightly shortens by 0.025 Å, and two hydrogen atoms are separated by 1.981 Å. The calculated barrier is 20.14 kcal/mol and the s-SNi−H_2 → s-$SNiH_2$ reaction step is found to be endothermic by 20.06 kcal/mol. Therefore, s-$SNiH_2$ is an intermediate at the B3LYP/6-31G** level but is not likely to be a local minimum at higher theory levels. The IRC calculations at the B3LYP/6-31G** level of theory confirmed that s-TS0(S) connects the s-SNi−H_2 and s-$SNiH_2$ intermediates. From s-$SNiH_2$, the hydrogen atom can shift further from Ni to S to form s-HNiSH via a nonplanar transition state s-TS1-(S). According to its geometry at the B3LYP/6-31G** level, s-TS1(S) is a very early transition state. The B3LYP/6-31G**

IRC calculation confirmed the connection between s-$SNiH_2$ and s-HNiSH via the first order saddle point s-TS1(S). According to B3LYP/6-311+G(3df,2p) calculations, the energy of s-TS1(S) is slightly lower than that of s-$SNiH_2$. All these results indicate that there is only one transition state and no local minima in the vicinity of s-TS0(S), s-$SNiH_2$, and s-TS1(S), as shown in Figure 4. If we take the energy of s-TS1(S) as the energy of this single TS, we find that it is slightly higher (by 1.1 kcal/mol) than the energy of t-TS1(S), so the triplet energy pathway to t-HNiSH is more favorable.

Triplet state is the ground electronic state for the HNiSH intermediate, it lies 5.7 kcal/mol lower than the singlet state. t-HNiSH decomposes to Ni(^{3}F) and H_2S via a nonplanar transition state t-TS2(S). At B3LYP/6-31G**, the Ni−S bond in t-TS2(S) (2.268 Å) becomes weaker and the hydrogen atom is shifted from the Ni side of the molecule to a position above the Ni−S bond, with S−H of 1.606 Å. The B3LYP/6-311+G-(3df,2p) calculations place transition state t-TS2(S) 26.8 kcal/mol higher in energy than t-HNiSH. The B3LYP/6-31G** IRC calculation confirmed that t-TS2(S) connects the t-HNiSH intermediate and the Ni(^{3}F) + H_2S products. On the other hand, from s-HNiSH, the reaction continues to form the s-Ni−SH_2 complex via a nonplanar transition state s-TS2(S). s-TS2(S) lies 13.9 kcal/mol above s-HNiSH at the B3LYP/6-311+G(3df,2p) level but 7.2 kcal/mol lower than t-TS2(S). The B3LYP/6-31G** IRC calculation confirmed that s-TS2(S) connects the s-HNiSH intermediate and the s-Ni−SH_2 complex. It takes 8.7 kcal/mol for the decomposition of s-Ni−SH_2 to Ni(^{1}D) + H_2S without an exit barrier. For the final reaction step, the singlet−triplet intersystem crossing taking place first between t-HNiSH and s-TS2(S) and then between the s-Ni−SH_2 complex and the Ni(^{3}F) + H_2S products is clearly important to enhance the reaction. Here, we did not locate the structure of the singlet−triplet intersection but can expect that the spin−orbit coupling in the vicinity of TS2(S) and s-Ni−SH_2 should be higher than for CI2 at the $NiOH_2$ surface since sulfur is heavier than oxygen.

Summarizing, the NiS + H_2 reaction begins on the triplet potential energy surface and proceeds via t-TS1(S) overcoming the barrier of ∼19 kcal/mol relative to NiS($^3\Sigma^-$) + H_2 to produce the global minimum—the HNiSH molecule in triplet electronic state, 18.2 kcal/mol below the reactants. This intermediate dissociates to the triplet Ni atom and H_2S via s-TS2(S) and the s-Ni−SH_2 complex involving singlet−triplet intersections. The energy of the intersystem crossing located between s-Ni−SH_2 and the triplet products would determine the exit barrier or the barrier for the reverse Ni(^{3}F) + H_2S reaction. Judging from the triplet−singlet energy splitting for the Ni atom (about 10 kcal/mol[25]), the energy of the intersystem crossing point is not expected to be high. Therefore, the t-Ni + H_2S reaction should be fast to yield the HNiSH molecule. The latter can, in turn, dissociate to NiS + H_2 overcoming a barrier of ∼37 kcal/mol relative to HNiSH or ∼13 kcal/mol with respect to the reactants. Thus, at elevated temperatures Ni atoms are expected to readily react with H_2S producing nickel sulfide and molecular hydrogen. The calculated heat of the NiS($^3\Sigma^-$) + H_2 → Ni(^{3}F) + H_2S reaction is 6.0 kcal/mol at the B3LYP/6-311+G(3df,2p) level, underestimating the experimental reaction endothermicity of 12.5 kcal/mol.[41]

D. Comparison of the NiO and NiS Reactions with Molecular Hydrogen. Although the reaction mechanisms of NiO and NiS with H_2 are similar, the energetics of the two reactions is quite different. For instance, the NiO + H_2 → Ni + H_2O reaction is 27 kcal/mol exothermic, while NiS + H_2 → Ni + H_2S is ∼12 kcal/mol endothermic. This is related to the fact that the heat of formation of H_2S is much higher (by ∼53 kcal/mol) than that of water, while the Ni−S bond is only ∼7 kcal/mol weaker than Ni−O. Both NiO and NiS can form molecular complexes with H_2 in singlet electronic state bound by 6−9 kcal/mol, while in the ground triplet electronic state such complexes are weaker (bound by 3−4 kcal/mol). The reactions can lead to the HNiOH and HNiSH molecules overcoming barriers in the range of 13−19 kcal/mol. The HNiOH and HNiSH intermediates have triplet ground electronic state, 6−9 kcal/mol below the singlet state. t-HNiOH is expected to be a much more stable intermediate (44.8 kcal/mol below the reactants) than t-HNiSH (only 18.2 kcal/mol below the reactants). These intermediates dissociate to nickel atoms and water or H_2S via the molecular complexes t-Ni−OH_2 or s-Ni−SH_2. For the oxygen case, triplet is the ground electronic state of the complex but for sulfur the complex exists only in the singlet state. For the Ni−OH_2 complex, the singlet electronic state also has a local minimum, 5.9 kcal/mol higher than t-Ni−OH_2, and stabilized only by 0.9 kcal/mol relative to Ni(^{1}D) + H_2O. Another common feature of the two reactions is the importance of the intersystem crossing and singlet−triplet transitions along the reaction pathway.

For the reverse reactions of Ni atoms with H_2O and H_2S, our calculations show that they can occur readily with relatively low activation barriers due to the singlet−triplet intersystem crossing on the pathway from the reactants to the t-HNiOH or the s-Ni−SH_2 complex. Both reactions produce stable HNiOH and HNiSH molecules lying 15−24 kcal/mol below the reactants. For the H_2S case, this intermediate can dissociate to NiS and H_2 with the barrier of ∼13 kcal/mol with respect to the initial reactants. For H_2O, the barrier to produce nickel oxide and molecular hydrogen is much higher, ∼43 kcal/mol. Therefore, it is not surprising that the experimental study of the gas-phase reaction of Ni atoms with water did not produce any evidence for the formation of NiO + H_2. Instead, the insertion product t-HNiOH was formed.[22]

In our previous studies,[8,9] we suggested the use of metal oxides and sulfides for reversible storage of molecular hydrogen. For instance, BeO and BeS can react with H_2 producing first molecular complexes with H_2, which then rearrange to HBeOH or HBeSH with low barriers. These compounds can be stored and, when necessary, selectively release H_2 because the energy barriers for Be + H_2O or Be + H_2S dissociation are significantly higher than those for the hydrogen release. One of the goals of the present study was to test a similar possibility for NiO and NiS. However, the calculations show that the energy barriers for the release of H_2O and H_2S from HNiOH and HNiSH are lower than those for the H_2 elimination. Interestingly, in the HNiSH system the Ni(^{3}F) + H_2S products lie higher in energy than NiS + H_2, however, the energetic order of the corresponding barriers is reverse.

4. Conclusions

The reaction of the nickel oxide with molecular hydrogen is demonstrated to involve both triplet and singlet potential energy surfaces. If the singlet−triplet intersystem crossing is efficient, the minimal energy reaction pathway includes the following steps. The reaction starts from the formation of the t-ONi−H_2 complex bound by 3.7 kcal/mol relative to NiO($^3\Sigma^-$) and H_2. Then, an intersystem crossing takes place (the spin−orbit-coupling calculated at a representative point CI1 of the singlet−triplet intersection is 86 cm^{-1}), and the system proceeds via the barrier of 13.3 kcal/mol at s-TS1 in singlet electronic state. Next, the HNiOH intermediate is formed in singlet or triplet

state. t-HNiOH, 9.1 kcal/mol more stable than s-HNiOH, lies 44.8 kcal/mol below the reactants and its formation involves another intersystem crossing. The HNiOH molecule rearranges to the triplet t-Ni−OH_2 molecular complex via transition state s-TS2 on the singlet potential energy surface and this process involves intersystem crossings in the transition state vicinity. CI2, a representative structure where the singlet and triplet surfaces cross, has the spin−orbit coupling of 27 cm^{-1}. On the last reaction step, the t-Ni−OH_2 complex dissociates to Ni(^{3}F) + H_2O without an exit barrier. For the reverse reaction, Ni(^{3}F) + H_2O → t-HNiOH, the barrier, 12.1 and 4.9 kcal/mol at the B3LYP/6-311+G(3df,2p) and CCSD(T)/6-311+G(3df,2p) levels, respectively, occurs at s-TS2 in singlet electronic state. The singlet and triplet surfaces cross along the reaction course and the singlet−triplet transitions significantly reduce the reaction barriers.

The NiS + H_2 reaction exhibits a similar scenario but different energetics. It begins on the triplet potential energy surface and proceeds via the barrier [at t-TS1(S)] of 19 kcal/mol relative to NiS($^3\Sigma^-$) + H_2 to produce the global minimum−the triplet HNiSH molecule, ∼18 kcal/mol below the reactants. This intermediate dissociates to the triplet Ni atom and H_2S via s-TS2(S) and the s-Ni−SH_2 complex involving two singlet−triplet transitions. The energy of the intersystem crossing located between s-Ni−SH_2 and the triplet products would determine the exit barrier and the barrier for the reverse Ni(^{3}F) + H_2S reaction. This reaction is predicted to rapidly produce the HNiSH molecule, which, in turn, can dissociate to NiS + H_2 overcoming the barrier of ∼37 kcal/mol relative to the intermediate or 13 kcal/mol with respect to the reactants. Since the highest barriers along the NiO + H_2 → Ni + H_2O and NiS + H_2 → Ni + H_2S reaction pathways are ∼13 and ∼19 kcal/mol, molecular hydrogen is expected to reduce nickel oxide and NiS to atomic nickel at elevated temperatures.

Acknowledgment. Funding from Tamkang University was used to buy the computer equipment used in part of this investigation. A partial support from Academia Sinica and from the National Science Council of Taiwan, R.O.C., is also appreciated.

References and Notes

(1) Kubas, G. J. *Acc. Chem. Res.* **1988**, *21*, 120.
(2) Crabtree, R. H. *Acc. Chem. Res.* **1990**, *23*, 95.
(3) Valtazanos, P.; Nicolaides, C. A. *Chem. Phys. Lett.* **1990**, *172*, 254.
(4) Nicolaides, C. A.; Valtazanos, P. *Chem. Phys. Lett.* **1990**, *174*, 489.
(5) Simandiras, E. D.; Nicolaides, C. A. *Chem. Phys. Lett.* **1991**, *185*, 529.
(6) Nicolaides, C. A.; Valtazanos, P. *Chem. Phys. Lett.* **1991**, *176*, 239.
(7) Valtazanos, P.; Nicolaides, C. A. *J. Chem. Phys.* **1993**, *98*, 549.
(8) Hwang, D.-Y.; Mebel, A. M. *Chem. Phys. Lett.* **2000**, *321*, 95.
(9) Hwang, D.-Y.; Mebel, A. M. *J. Am. Chem. Soc.* **2000**, *122*, 11406.
(10) Kauffman, J. W.; Hauge, R. H.; Margrave, J. L. *J. Phys. Chem.* **1985**, *89*, 3541; 3547.
(11) Park, M.; Hauge, R. H.; Margrave, J. L. *High Temp. Sci.* **1988**, *25*, 1.
(12) Hudgins, D. M.; Porter, R. F. *Rapid Commun. Mass Spectrom.* **1988**, *2*, 197.
(13) Parks, E. K.; Winter, B. J.; Klots, T. D.; Riley, S. J. *J. Chem. Phys.* **1991**, *94*, 1882.
(14) Callen, B. W.; Griffiths, K.; Norton, P. R.; Harrington, D. A. *J. Phys. Chem.* **1992**, *96*, 10905.
(15) Blomberg, M. R. A.; Brandemark, U. B.; Siegbahn, P. E. M.; Mathisen, K. B.; Karlström, G. *J. Phys. Chem.* **1985**, *89*, 2171.
(16) Bauschlicher, C. W., Jr. *J. Chem. Phys.* **1986**, *84*, 260.
(17) Sauer, J.; Haberlandt, H.; Pacchioni, G. *J. Phys. Chem.* **1986**, *90*, 3051.
(18) Haberlandt, H.; Sauer, J.; Pacchioni, G. *J. Mol. Struct. (THEOCHEM)* **1987**, *149*, 297.
(19) Blomberg, M. R. A.; Brandemark, U. B.; Siegbahn, P. E. M. *Chem. Phys. Lett.* **1986**, *126*, 317.
(20) Bauschlicher, C. W., Jr. *Chem. Phys. Lett.* **1987**, *142*, 71.
(21) Blomberg, M. R. A.; Schúle, J.; Siegbahn, P. E. M. *J. Am. Chem. Soc.* **1989**, *111*, 6156.
(22) Mitchell, S. A.; Blitz, A.; Siegbahn, P. E. M.; Svensson, M. *J. Chem. Phys.* **1994**, *100*, 423.
(23) Fournier, R. *Theor. Chim. Acta* **1995**, *91*, 129.
(24) Hwang, D. Y.; Mebel, A. M. *J. Phys. Chem. A* **2001**, *105*, 10433.
(25) Moore, S. E. *Atomic Energy Levels*; NSRDS: Washington, D. C., 1971.
(26) Wu, H.; Wang, L.-S. *J. Chem. Phys.* **1997**, *107*, 16.
(27) Becke, A. D. *J. Chem. Phys.* **1993**, *98*, 5648.
(28) Lee, C.; Yang, W.; Parr, R. G. *Phys. Rev. B* **1988**, *37*, 785.
(29) Hehre, W. J.; Radom, L.; Schleyer, P. v. R.; Pople, J. A. *Ab Initio Molecular Orbital Theory*; Wiley: New York, 1986.
(30) Gonzalez, C.; Schlegel, H. B. *J. Phys. Chem.* **1990**, *94*, 5523.
(31) Purvis, G. D.; Bartlett, R. J. *J. Chem. Phys.* **1982**, *76*, 1910.
(32) (a) Werner, H.-J.; Knowles, P. J. *J. Chem. Phys.* **1985**, *82*, 5033. (b) Knowles, P. J.; Werner, H.-J. *Chem. Phys. Lett.* **1985**, *115*, 259.
(33) (a) Werner, H.-J.; Knowles, P. J. *J. Chem. Phys.* **1988**, *89*, 5803. (b) Knowles, P. J.; Werner, H.-J. *Chem. Phys. Lett.* **1988**, *145*, 514.
(34) Frisch, M. J.; Trucks, G. W.; Schlegel, H. B.; Scuseria, G. E.; Robb, M. A.; Cheeseman, J. R.; Zakrzewski, V. G.; Montgomery, J. A., Jr.; Stratmann, R. E.; Burant, J. C.; Dapprich, S.; Millam, J. M.; Daniels, A. D.; Kudin, K. N.; Strain, M. C.; Farkas, O.; Tomasi, J.; Barone, V.; Cossi, M.; Cammi, R.; Mennucci, B.; Pomelli, C.; Adamo, C.; Clifford, S.; Ochterski, J.; Petersson, G. A.; Ayala, P. Y.; Cui, Q.; Morokuma, K.; Malick, D. K.; Rabuck, A. D.; Raghavachari, K.; Foresman, J. B.; Cioslowski, J.; Ortiz, J. V.; Baboul, A. G.; Stefanov, B. B.; Liu, G.; Liashenko, A.; Piskorz, P.; Komaromi, I.; Gomperts, R.; Martin, R. L.; Fox, D. J.; Keith, T.; Al-Laham, M. A.; Peng, C. Y.; Nanayakkara, A.; Gonzalez, C.; Challacombe, M.; Gill, P. M. W.; Johnson, B.; Chen, W.; Wong, M. W.; Andres, J. L.; Head-Gordon, M.; Replogle, E. S.; Pople, J. A. *Gaussian 98*, Revision A.7; Gaussian, Inc.: Pittsburgh, PA, 1998.
(35) MOLPRO is a package of ab initio programs written by H.-J. Werner and P. J. Knowles, with contributions from Almlöf, J., Amos, R. D., Deegan, M. J. O., Elbert, S. T., Hampel, C., Meyer, W., Peterson, K., Pitzer, R., Stone, A. J., Taylor, P. R., and Lindh, R.
(36) (a) Green, D. W.; Reedy, G. T.; Kay, J. G. *J. Mol. Spectrosc.* **1979**, *78*, 257. (b) Srdanov, V. I.; Harris, D. O. *J. Chem. Phys.* **1988**, *89*, 2748. (c) Ram, R. S.; Bernath, P. F. *J. Mol. Spectrosc.* **1992**, *155*, 315. (d) Namiki, K.; Saito, S.; *Chem. Phys. Lett.* **1996**, *252*, 343. (c) Bakalbassis, E. G.; Stiakaki, M. A. D.; Tsipis, A. C.; Tsipis, C. A. *Chem. Phys.* **1996**, *205*, 389.
(37) Bauschlicher, C. W., Jr.; Maitze, P. *Theor. Chim. Acta* **1995**, *90*, 189.
(38) Citra, A.; Chertihin, G. V.; Andrews, L.; Neurock, M. *J. Phys. Chem. A* **1997**, *101*, 3109.
(39) Doll, K.; Dolg, M.; Fulde, P.; Stoll, H. *Phys. Rev. B* **1997**, *55*, 10282.
(40) Watson, L. R.; Thiem, T. L.; Dressler, R. A.; Salter, R. H.; Murad, A. *J. Phys. Chem.* **1993**, *97*, 5577.
(41) *CRC Handbook of Chemistry and Physics*, 75 ed.; Lide, D. R., Ed.; Chemical Rubber: Boca Raton, FL, 1995.
(42) Cui, Q. Ph.D. Thesis, Emory University, Atlanta, 1998. Some details of the algorithm are described in Dunn, K.; Morokuma, K. *J. Chem. Phys.* **1995**, *102*, 4904. The program uses the HONDA package by M. Dupuis.
(43) Brown, C. E.; Mitchell, S. A.; Hackett, P. A.; *Chem. Phys. Lett.* **1992**, *191*, 175.
(44) Brown, C. E.; Blitz, M. A.; Decker, S. A.; Mitchell, S. A. In *Laser Chemistry of Organometallics*; Chaiken, J., Ed.; American Chemical Society Symposium Series 530, American Chemical Society: Washington, DC, 1993; Chapter 14.